



Supplement of

Contrasts in the marine inorganic carbon chemistry of the Benguela Upwelling System since the Last Glacial Maximum

Szabina Karancz et al.

Correspondence to: Szabina Karancz (szabina.karancz@nioz.nl)

The copyright of individual parts of the supplement might differ from the article licence.

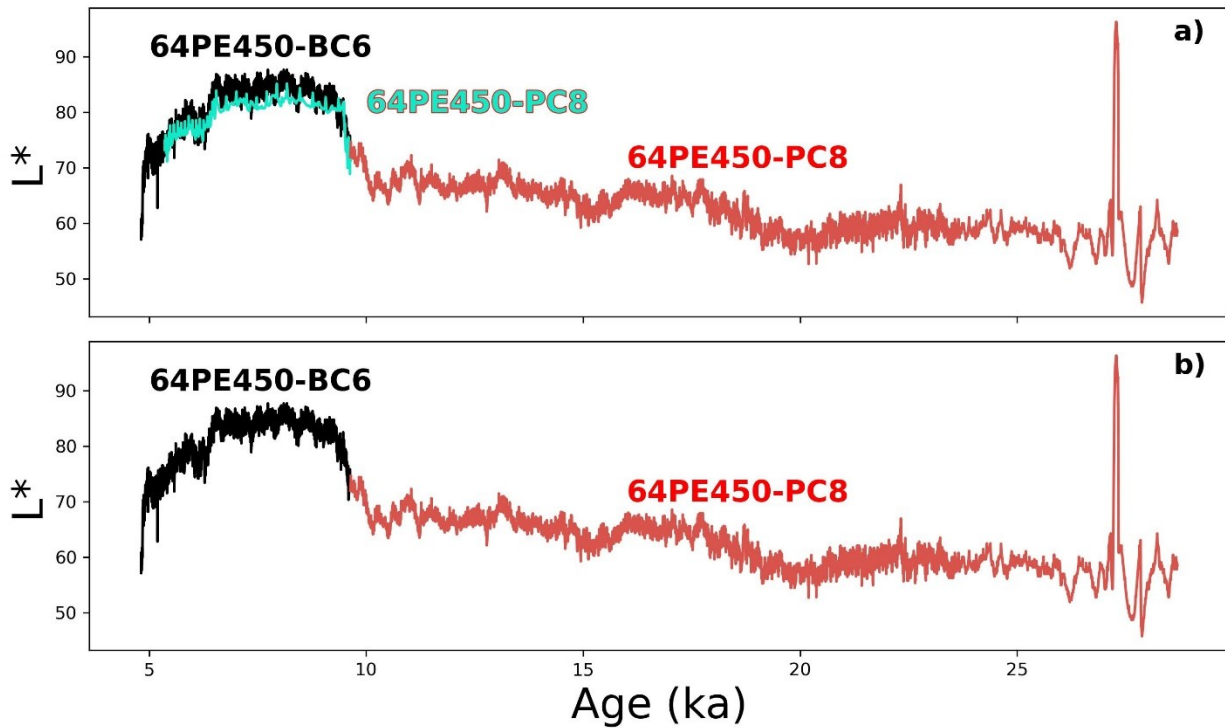


Figure S1. Light reflectance (L^*) measured in sediment cores 64PE450-BC6 (black line) and 64PE450-PC8 (red and green lines) plotted over the last 29 kyr. Panel a) shows the record including the overlap of 64PE450-BC6 with the top 4.24 cm of 64PE450-PC8, which has been excluded from this study due to sediment disturbance likely caused by the coring technique used (green line). Panel b) shows the alignment of 64PE450-BC6 and 64PE450-PC8 that produces a near continuous record from 27 to 4.8 ka.

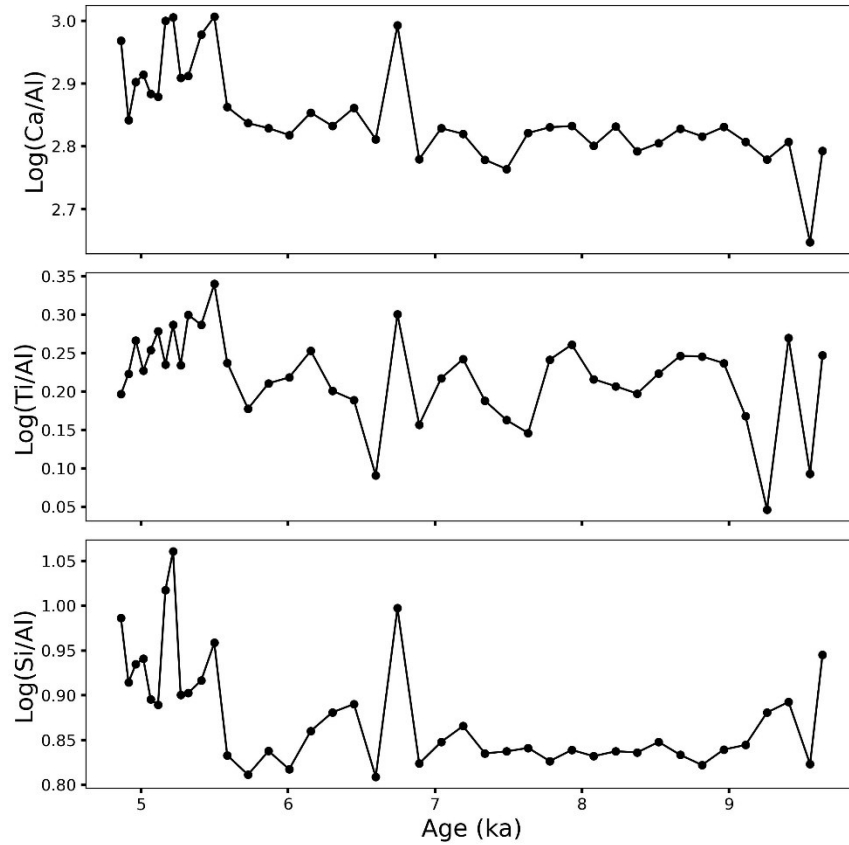


Figure S2. Log(Ca/Al), Log(Ti/Al), and Log(Si/Al) ratios (XRF-scanning element intensities) of 64PE450-BC6 plotted over the last 10 kyr. The geochemical composition of the sediment was acquired through X-Ray Fluorescence (XRF)-core-scanning using an Avaatech scanner at the Royal Netherlands Institute of Sea Research (NIOZ). The data was obtained at 1-cm resolution using a 10kV energy setting with a current of 0.6 mA and a measurement time of 10 seconds. We show the data as log-ratios of intensities, as they provide the easiest interpretable signals of relative chemical composition change (Weltje and Tjallingii, 2008).

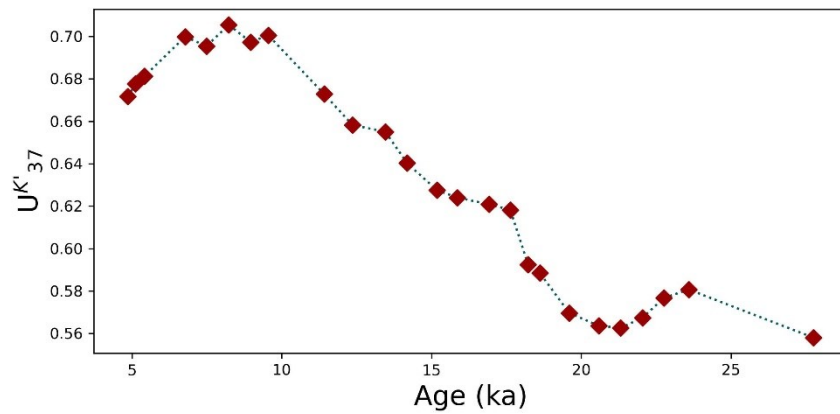


Figure S3. Ketone unsaturation index ($U^{K'}_{37} = C_{37:2} / (C_{37:3} + C_{37:2})$; Prahl and Wakeham, 1987) plotted over the past 27.8 kyr.

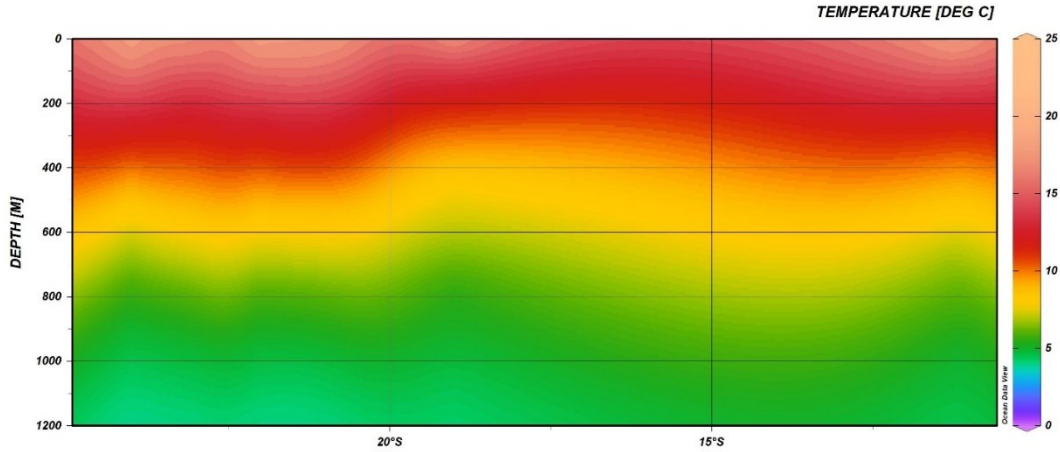


Figure S4. Depth transect in the northern Benguela Upwelling System showing temperature distribution. Temperature values are obtained from GLODAPv2023 (Lauvset et al., 2024; Olsen et al., 2016; Key et al., 2015).

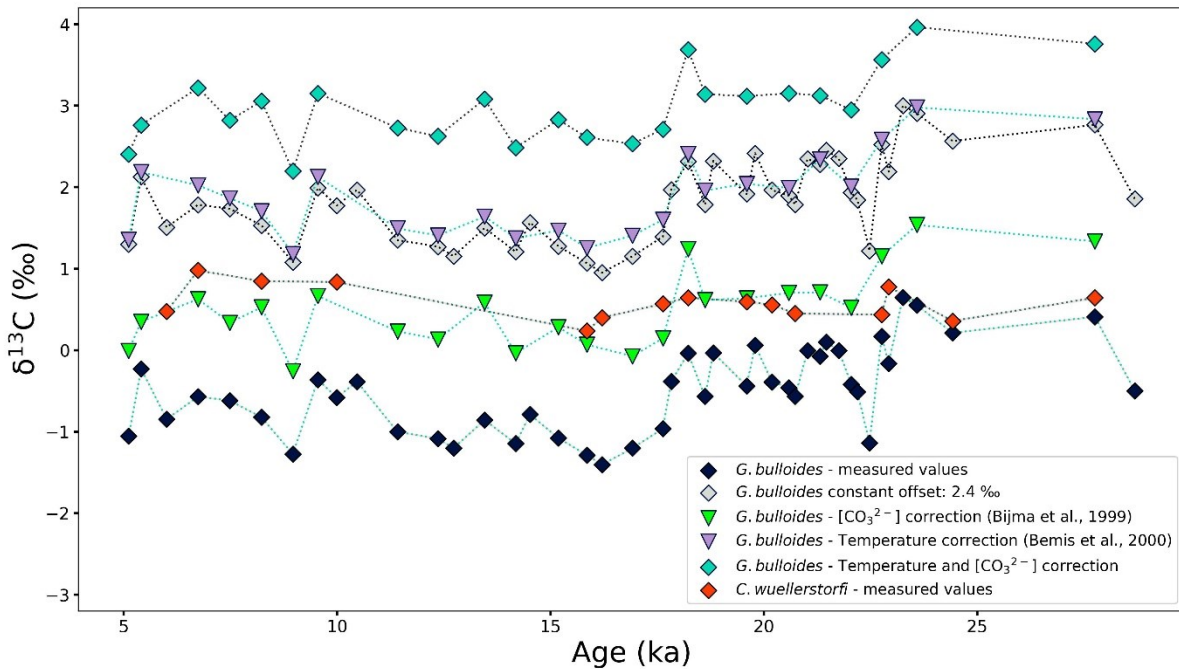


Figure S5. Measured $\delta^{13}\text{C}$ values of *G. bulloides* (dark blue diamonds), and *C. wuellerstorfi* (red diamonds), and $\delta^{13}\text{C}$ values of *G. bulloides* corrected for temperature (purple triangles; Bemis et al., 2000), $[\text{CO}_3^{2-}]$ (green triangles; Bijma et al., 1999), and for a constant offset of 2.4 ‰ (grey diamonds, corresponding to the modern offset to $\delta^{13}\text{C}$ of DIC) plotted over the past 27.8 kyr. Green diamonds display $\delta^{13}\text{C}$ values corrected for both temperature (derived from Mg/Ca; Bemis et al., 2000) and $[\text{CO}_3^{2-}]$ (derived from pH and TA; Bijma et al., 1999).

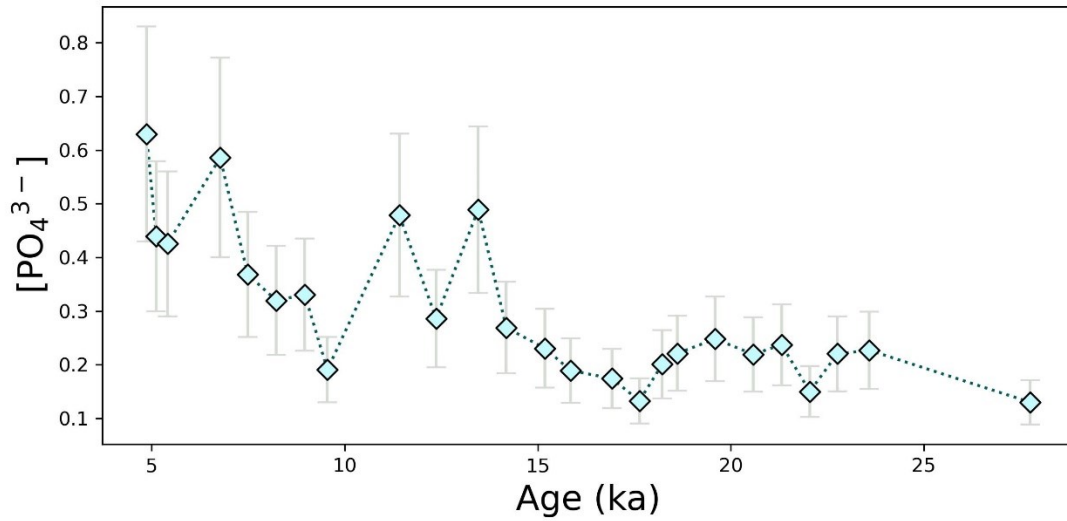


Figure S6. Estimated concentrations of PO_4^{3-} based on foraminiferal Ba/Ca ratios (e.g., Hönisch et al., 2011; Lea and Spero, 1994) over the last 27.8 kyr.

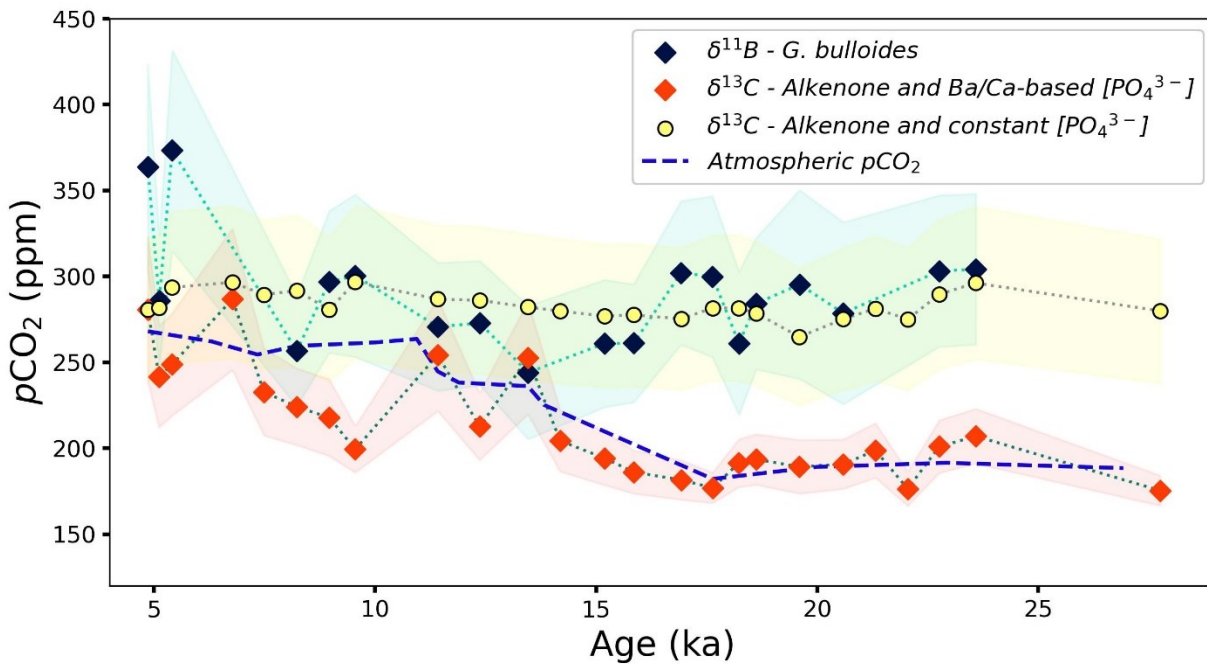


Figure S7. Comparison of $p\text{CO}_2$ reconstructions using $\delta^{13}\text{C}$ of alkenones combined with constant $[\text{PO}_4^{3-}]$ (yellow circles) and with Ba/Ca-based $[\text{PO}_4^{3-}]$ reconstruction (red diamonds). Blue diamonds show $p\text{CO}_2$ reconstruction based on $\delta^{11}\text{B}$ of *G. bulloides* and constant total alkalinity, and blue dashed line indicates atmospheric $p\text{CO}_2$ from the Vostok ice core record (Petit et al., 1999).